

ISTITUTO NAZIONALE DI FISICA NUCLEARE

Sezione di Torino

INFN/FM-86/1  
16 Ottobre 1986

**C. Manfredotti, A. Gabutti, G. Gervino, E. Monticone and U. Nastasi:  
STUDY ON HgI<sub>2</sub> NUCLEAR DETECTOR**

**INFN - ISTITUTO NAZIONALE DI FISICA NUCLEARE**

Sezione di Torino

**INFN/FM-86/1**

**16 Ottobre 1986**

**STUDY ON HgI<sub>2</sub> NUCLEAR DETECTOR.**

C. Manfredotti, A. Gabutti, G. Gervino, E. Monticone and U. Nastasi  
Istituto di Fisica Superiore dell'Universita' di Torino  
and I.N.F.N. Sezione di Torino

**ABSTRACT**

In this paper we discuss the electrical characteristics, the present "state of-the-art", the analysis of trapping and detrapping phenomena and the results of our investigations on HgI<sub>2</sub> crystal. We present also a calculation of the carrier drift-mobility, both cutting the crystal parallel and perpendicular to c-axis. Some X and gamma spectra obtained are presented and discussed with an evaluation of the total noise of our detection set-up.

**1. - INTRODUCTION**

The wide bandgap of mercuric iodide in combination with the high atomic number of this compound makes it an attractive material as semiconductor nuclear detector which operates at room temperature.

Most studies performed with HgI<sub>2</sub> and reported in literature<sup>(1-5)</sup>, deal with the spectroscopic behaviour of HgI<sub>2</sub> detector when irradiated with radioisotopes which emit gamma or X-ray yielding low fluences of up to 10<sup>4</sup> photons sec.<sup>-1</sup> cm<sup>-2</sup>.

At present poor carrier mobility, for holes in particular ( $\mu = 4$  cm<sup>2</sup> / V\*sec) and poor hole collection (we have estimated an upper-limit hole efficiency

collection  $\eta = 0.752$ ), are serious limitations for high energy photon spectroscopy.

We have carried out systematic measurements on electrical characteristics, polarization effect, trap density and photoconduction in order to evaluate  $\text{HgI}_2$  as useful radiation detector, besides we have investigated new way of arrangement for improving its performances, above all to overcome its poor hole mobility.

This report presents the results of our research finalized to study the possibility of  $\text{HgI}_2$  applications in relatively new fields, as a survey dosimeter with a very good sensivity and spatial resolution<sup>(6)</sup>.

## 2. - EXPERIMENTAL

The  $\text{HgI}_2$  crystals investigated in this work have been extracted from ingots grown by T.O.M. technology (temperature oscillating method) in a vertical furnace<sup>(7)</sup>. Crystals of  $1 \text{ cm}^2$  surface area and thicknesses ranging from  $200 \mu\text{m}$  to  $900 \mu\text{m}$  have been used. Thickness uniformity of each platelets has been controlled with a short etching in 20 % KI solution. The electrodes are realized on each platelet surface by vacuum evaporation of a thin film of Pd or gold ( $500 \text{ \AA}$ ) and upon a  $25 \mu\text{m}$  thickness silver wire is bonding by Hydrocollag (sandwich arrangement) Sample surface are passived by insulating and protective coating HumiSeal.

## 3. - PHOTOELECTRONIC PROPERTIES

Photoelectronic techniques have been widely used for  $\text{HgI}_2$ , which is a good photoconductor, in the early stages of its developement, in order to evaluate its performances as an X-ray detector. We lighted the detector by a photon

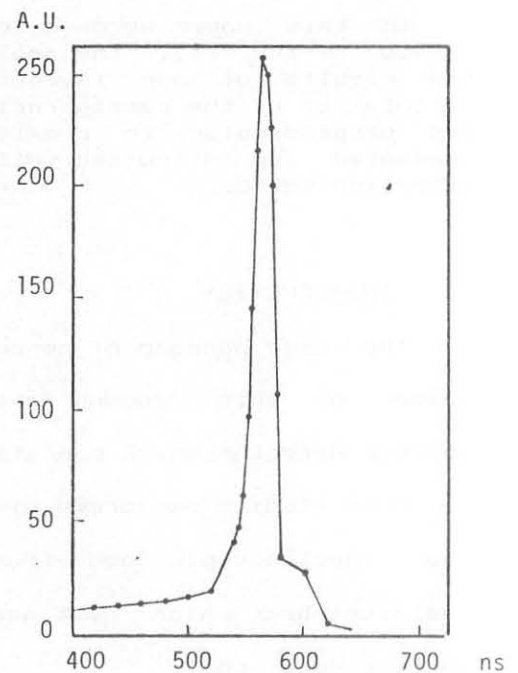


FIG.1-Spectral response of photoconductivity for the sample N-8-2 at 23 C.

monochromatic beam of about  $1-3 \mu\text{Watt}/\text{cm}^2$  coming out from a Xenon lamp and Optics MC1-04 minimonochromator (resolution of about  $10 \text{ \AA}$ ) and we measured the photocurrent in function of the wavelength. In Fig.1 it is shown the excitonic peak which we have found as spectral response of the photoconductivity, in good agreement with the measurements of ref.8-9. No particular differences were found with respect to the thickness of the samples which was used, and to the luminous intensity at least as far as the general behaviour of the effect as a function of the wavelength. The shape of the excitonic peak gives also a good indication of both chemical and cristallographic purity of the detector.

#### 4. - ELECTRICAL CHARACTERISTICS

In Fig.2 it is shown an I-V characteristic of a  $350 \mu\text{m}$  thickness  $\text{HgI}_2$  sample, cut ortogonally to cristallographic-axis. Before taking the measurements we have polarized the samples during 24 hours with 900 volt bias voltage to reach the steadiest condition. The first section of the I-V characteristic is, with a good approximation, ohmic, then around 400 volt the curve clearly changes its slope. The reason of this effect remains till now obscure. As the bias voltage is stepped up, working where the I-V characteristic is ohmic to be sure to avoid injection effect

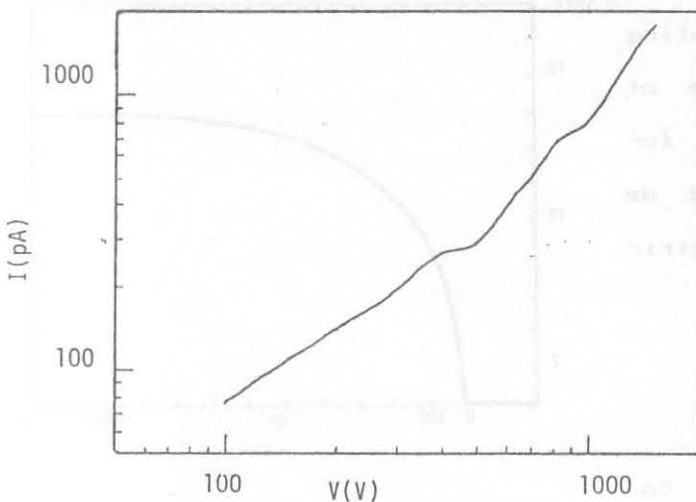


FIG.2: I-V Log-Log characteristic of  $350 \mu\text{m}$  sample cut ortogonally to c-axis

from electrodes and SCLC phenomena, the current at first increases and then decays with a time constant varying from 1 to 1000 sec. By integrating this trap charging current (the value obtained has, of course, a dimension of a charge) we have estimated the trap density of about  $10^{14} \text{ cm}^{-3}$ .

We have taken I-V characteristics from samples with

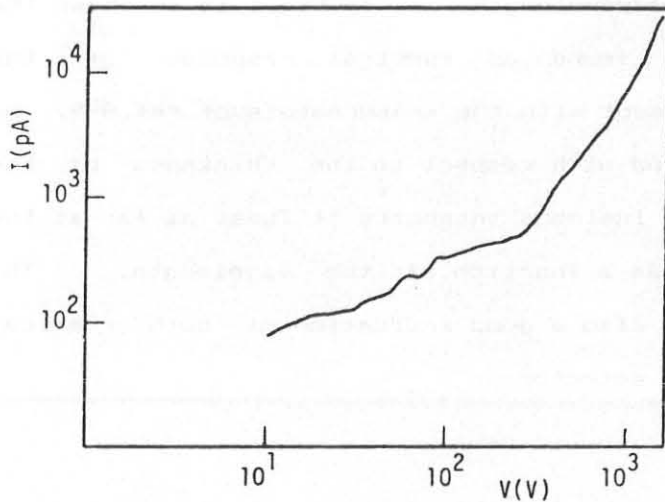


FIG. 3: I-V Log-Log characteristic of 880  $\mu\text{m}$  thick  $\text{HgI}_2$  cut perpendicularly to the layers.

thickness  $\text{HgI}_2$  platelet, cut perpendicularly to the layers using an acid saw fed by 10% KI solution.

The measured dark current is roughly higher, compared to Fig.2. Using an acid saw, we make relevant irregularity on the  $\text{HgI}_2$  surface (about 50  $\mu\text{m}$  after a good etching in KI solution) and this is surely the cause of an inhomogenous electric field with associated point-effects that carry in charge injections. Ions  $\text{K}^+$  may either get exchanged with Hg or diffuse into the crystal.

C-V measurements on operating detectors showed no dependence of capacitance on bias voltages for fields up to  $8.1 \times 10^4$  V/cm. and we have a value for the dielectric constant of  $\epsilon_r = 9.1$ .

5. = CARRIER MOBILITY

$\text{HgI}_2$  detectors were exposed to collimated alpha particles of an Am-241 source in a vacuum chamber

three different types of electrodes: palladium, carbon and gold. We have not noticed any relevant difference between samples with carbon or palladium contacts, but the samples with gold contacts have a very high dark current: it seems that gold contacts cause a strong charge injection, also at relatively low bias voltage.

In Fig.3 it is shown an I-V characteristic of a 880  $\mu\text{m}$

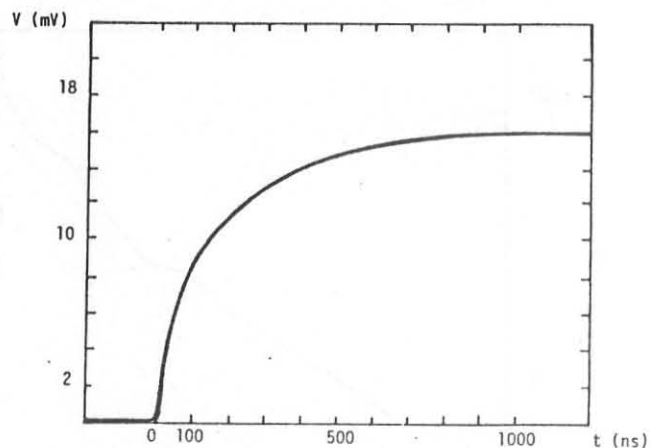


FIG.4: Electronic signal coming from Seforad SR 205 fast preamp. exposing  $\text{HgI}_2$  detector cut parallel to c-axis at an Am-241 alpha source.

and the pulses coming from a fast preamplifier Seforad Mod. SR 205 were recorded by a storage CRT. The pulse rise-time was accurately measured by tracking the tangent to the pulse in its origin on the time axis (Fig.4). From the relation

$$\mu = \left. \frac{dQ}{dt} \right|_{t=0} * \frac{d}{EQ} \quad (1)$$

where  $\left. \frac{dQ}{dt} \right|_{t=0}$  is equal to the pulse rise-time tangent,  $d$  is the

distance by the electrodes and we calculated  $Q_0$ , considering the pulse height after a long time to permit the detrapped charge to be collected, we measured the drift mobility of electrons and holes in the directions parallel and perpendicular to c-axis; all the results obtained are shown in Tab.1 together with the results quoted in literature and obtained not only by the time of flight method<sup>(10)</sup>, but also by PME effect (ref.11). The comparison of values quoted in the first three columns can give an either good check of the precision of the method used. The values are the maximum

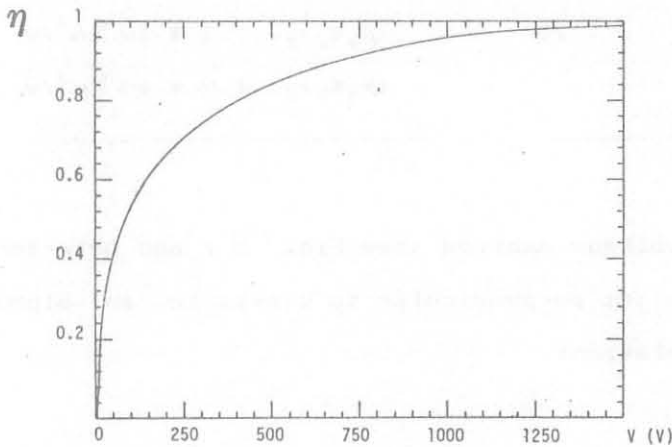


FIG.5: Charge collection efficiency vs. bias voltage of a 350  $\mu\text{m}$   $\text{HgI}_2$  detector exposed to 5.4 MeV particles. We can see that  $d\eta/dE$ , for  $E = 0$ , very well fits the curve as far as  $E = 3 * 10^3$  V/cm

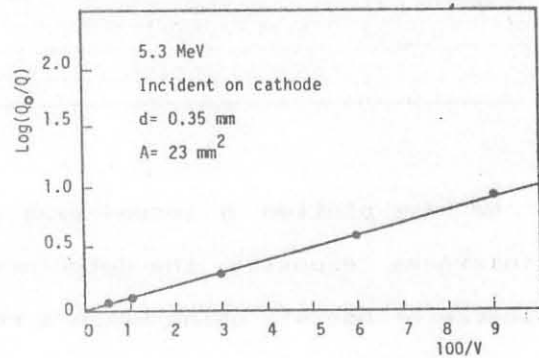


FIG.6: Pulse rise-time and normalized charge collection as a function of bias in  $\text{HgI}_2$  detector N - 8 - 2 for alpha particles.

ones which have been obtained, however fluctuations among the various samples were no more than few percents as far as electron mobilities are concerned. Hole mobility fluctuations are more heavily from sample to sample: particularly varied from 9 up to 19  $\text{cm}^2\text{V}^{-1}\text{sec}^{-1}$ . This fact can be easily

attributed to different damages introduced into the samples by cutting operation and the highest value can be safely considered as a representative value for hole mobility in our samples. The fact that hole mobility along the layer is higher than along c-axis is a fact that strongly differentiates HgI<sub>2</sub> with respect to other layer compounds<sup>(10)</sup> and even if it should be likely attributed to different scattering mechanisms for electrons and holes in HgI<sub>2</sub>, its origin remains relatively obscure at this point. We have carried out systematic measurements of  $\mu\tau$  product for both carriers, cutting the crystals parallel and orthogonally to c-axis, following different methods (see Tab. II).

Tab. I

Comparison of values of electron  $\mu_e$  and hole  $\mu_h$  drift mobility obtained by present work, by T.O.F.<sup>(4)</sup> and P.E.M.<sup>(5)</sup> method.

Mobility (cm <sup>2</sup> V <sup>-1</sup> sec <sup>-1</sup> )	$\mu_{\parallel}$	$\mu_{\perp}$	$\mu_{\parallel}$	$\mu_{\perp}$
Present work	101	67	4.5	19
T.O.F.	100	65	4.0	-
P.E.M.	-	-	-	23

Tab. II

$\mu\tau$  calculation for holes and electrons, for detector cut and to c-axis.

$(\mu_e \tau_e)_{\perp}$	$4 * 10^{-5} \text{ cm}^2 / \text{V}$
$(\mu_h \tau_h)_{\perp}$	$6 * 10^{-6} \text{ cm}^2 / \text{V}$
$(\mu_e \tau_e)_{\parallel}$	$2 * 10^{-4} \text{ cm}^2 / \text{V}$
$(\mu_h \tau_h)_{\parallel}$	$1.2 * 10^{-5} \text{ cm}^2 / \text{V}$

We have plotted  $\eta$  versus bias voltage applied (see Fig. 5) and detector thickness exposing the detectors cut perpendicular to c-axis to an alpha source of Am-241, using Hetch's relation:

$$\eta = \frac{\mu\tau E}{d} * \left( 1 - e^{-\frac{d}{\mu\tau E}} \right) \quad (2)$$

where d is the detector thickness.

Calculating  $d\eta/dE$  for  $E=0$  and assuming, in good approximation, that  $d\eta/dE$  very well fits the curve from  $E=0$  up to  $E=3*10^3$  V/cm, we have found the hole mobility-lifetime product  $\mu_h\tau_h$  equal to  $1.2*10^5$  cm<sup>2</sup>/V.

Another method of determining transport and trapping parameters makes use of alpha particle spectra and charge-pulse shape analysis. Fig. 6 shows

the 0-90 % rise time,  $T_R$ , and the normalized charge collection,  $\ln(Q_0/Q)$ , as a function of  $100/V$  for electron transport at room temperature. The ratio  $Q_0/Q$  is determined from the alpha peak position in the spectrum.

Assuming the following hypothesis : a) electron trapping is assumed to have the dependence  $\exp(-t/\tau E)$ , b) detrapping is thought negligible and c) a uniform drift field exists in the  $HgI_2$  detector, then  $\mu_e \tau_e$  product may be determined directly from Fig.6. The injected charge decays as

$$Q(t) = Q_0 e^{-t / \tau_e} \quad (3)$$

where  $\tau_e^{-1} = (\tau^+)^{-1} + (\tau_0)^{-1}$ ,  $\tau^+$  is the trapping-time and  $\tau_0$  is the detrapping-time. With a transit time  $T_R = d/\mu E$  the collected charge may be expressed as

$$\ln \frac{Q_0}{Q} = \frac{d^2}{\mu_e \tau_e} \frac{1}{V} \quad (4)$$

Thus the slope of the line in Fig.6 is  $d^2/\mu_e \tau_e$ , and  $\mu_e \tau_e$  is  $2 \cdot 10^{-4} \text{ cm}^2/V$  for a detector cut perpendicularly to c-axis. For a detector cut parallel to c-axis we have found  $\mu_h \tau_h = 6.187 \cdot 10^{-6} \text{ cm}^2/V$  and  $\mu_e \tau_e = 4 \cdot 10^{-5} \text{ cm}^2/V$  (all these results are quoted in Tab.II) The electron trapping time may also be determined from the pulse shape of the fast rise-time component of the collected charge. If detrapping is neglected and a uniform field and trapping are assumed, the transient response is given by<sup>(12)</sup>:

$$Q(t) = Q \frac{\tau}{T_R} [1 - \exp(-t/\tau)] \quad (5)$$

$t \leq T_R$

This indicates that the trapping time may be determined from a plot of  $\ln[Q(\infty) - Q(t)]$  versus  $t$ . This is shown in Fig.7 where  $\tau$  is determined to be 300 nsec.

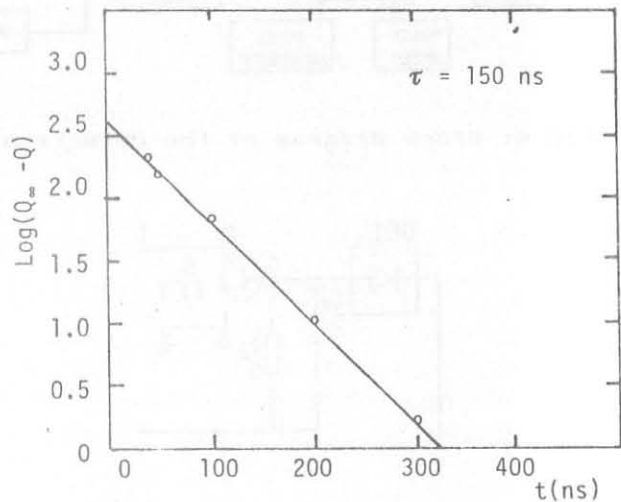


FIG.7: Charge pulse transient analysis used to determine electron trapping time for  $HgI_2$  sample N-8-2.



The differences between this value and the one determined by charge collection and transit time measurements ( 1980 nsec. against 300 ) may be an indication that the trapping and/or the electric field is not really uniform.

Since the pulse shape measurement at fixed bias is very dependent upon field and trapping homogeneity, the  $\mu\tau$  values based on charge collection are more meaningful.

6. - SPECTROSCOPY WITH HgI<sub>2</sub>

The number of pairs created in the semiconductor fluctuates following Poisson's statistic, and the energy resolution,  $\Delta E_f$ , considering only this effect is:

$$\Delta E_f = 2.35 \sqrt{FE\epsilon} \tag{6}$$

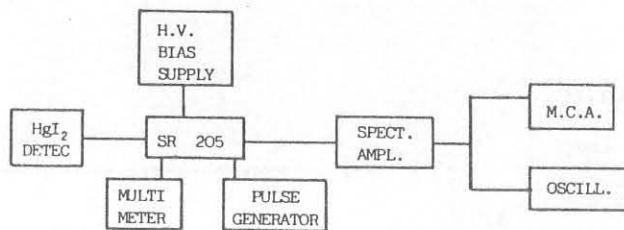


FIG.8: Block diagram of the detection set-up

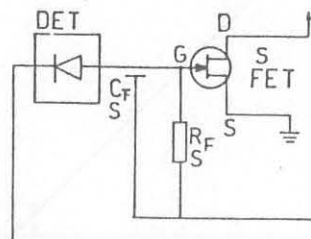


FIG.9: First stage of Seforad SR-205 preamplifier.

where F is the upper-limit Fano factor that for HgI<sub>2</sub> has been evaluated equal to 0.27<sup>(6)</sup> and  $\epsilon$  is the average energy to create a pair hole - electron ( 4.2 eV ). We have estimated that this effect contributes of the total FWHM of gamma and X-ray peaks in order to 8-13% in the energy range from 50-130 KeV and 10-50 KeV respectively.

The noise done by the incomplected charge collection  $\Delta E_C$  associated to the trapping effect, have evaluated using the empirical formula proposed by Henke<sup>(12)</sup>. Because in the case of HgI<sub>2</sub>  $\mu_e$  is strongly different from  $\mu_h$ ,  $\Delta E_C$  has not gaussian behaviour:

$$\Delta E_C = A ( 1 - \eta ) E_\gamma^{\frac{1}{2}} \tag{7}$$

(eV)

where  $E_\gamma$  is the incident energy in MeV and  $A$  is an empirical constant. At general Henke's formula is valuable only for a collection efficiency  $\eta$  equal to 0.99, and using this value it has been estimated  $A=4.7*10^5$ .

In Fig.8 it is shown a block diagram of the electronic chain used. In Fig.9 it is shown the first stage of the SR 205 SEFORAD preamplifier. The electronic noise of all the detection chain (electronic and  $HgI_2$  crystal) is given, following Radeka's formula, by :

$$(\Delta E_n)^2 = (\Delta E_{n_0})^2 + 1.18*10^3 I_d + 0.1 \frac{T}{\tau} r_s * (C_d^2 + 2C_d C_0) \quad (eV) \quad (8)$$

where  $\Delta E_{n_0}$  (eV) is the intrinsic noise of the preamplifier without detector,

$I_d$  (pA) is the detector reverse current,

$\tau$  (usec.) is the RC constant of time, assuming the integration and differentiation constant of time to be equal,

$T$  (°K) is the room temperature,

$r_s$  (ohm) is the equivalent resistance in series to the first stage of the preamplifier,

$C_d$  (pF) is the detector capacitance (in our case the detector is directly joined to the JFET of the preamplifier without any cable),

$C_0$  (pF) is the source-gate capacitance of the preamplifier first stage FET.

Obviously  $\Delta E_n$  is completely independent from the incident radiation and we have evaluated its value in the range from 850 up to 1100 eV depending from the capacitance of the detector. As the noise components are each other independents, the estimate of the total noise is given by:

$$(\Delta E)^2 = (\Delta E_f)^2 + (\Delta E_c)^2 + (\Delta E_n)^2 \quad (9)$$

and for a samples 350  $\mu m$  thick with a capacitance of 4.8 pF (at 1 MHz) and a reverse current equal to 680 pA at 900 V bias voltage, we have found  $E_{FWHM} = 2.9$  KeV as a theoretical value, in good agreement with the  $E_{FWHM} = 3.1$  KeV that we have found applying a pulse at our experimental apparatus (with the detector insert). In Fig. 10 it is shown the collection efficiency  $\eta$  versus the incoming radiation and we can notice that  $\eta$  varies rapidly at

low energy, in particular if the bias voltage is not too much high (below 150 Volt ). For an incident radiation upon 100 KeV becomes constant and depends only on the bias voltage, because the holes are not completely collected. In Fig. 11 we have plotted  $E_{FWHM}$  versus the incident radiation energy E. Our experimental curve is roughly different from the theoretical one<sup>(14)</sup> (see Fig. 12 ) and this can be attributed to the hole trapping effect and to the polarization effect. In the Co-57 gamma spectra

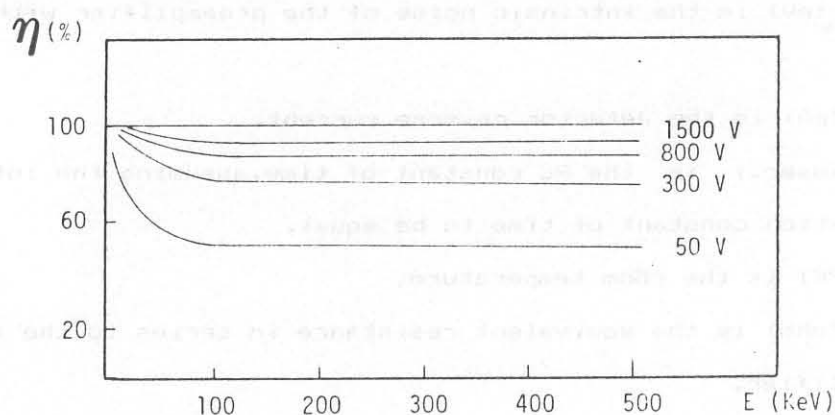


FIG.10: Collection efficiency in function of the incoming radiation E.

shown in Fig. 13 the photoelectric peak behaviour presents strong asymmetries, caused by the difference of the  $\mu\tau$  between holes and electrons. This difference involves a spatial variation in the collection efficiency that carry in an indetermination in the electronic signal high, and this is the principal cause of the FWHM of the peak. In low energy X spectra (Figs. 14 - 15 ) where the signal is due only to electron collection, we do not see any relevant asymmetry, so the photopeak is not widened by strong trapping effect. But also in this case the experimental FWHM is different from the theoretical value that we have a-priori calculated (i.e. in the case of Ba, in Fig. 15, we have an experimental FWHM of 5 KeV against a theoretical prediction of 2.9) and this fact suggests us that we are in presence of polarization effect. When the bias voltage is switched to

zero, after irradiating the detector, the polarity of the output reverses. This effect decays in about one minute until, finally, small pulse of both polarity are observed. This effect is a proof of the presence of an induced dipole electric field that is caused by electron traps that are filled when the voltage is applied and subsequently empty slowly at zero voltage bias. The presence of weak pulses of both polarity at zero bias indicate both contacts have a local electric field. From these facts we assume that a potential barrier is formed when the contacts are applied, giving rise to a positive space charge. In Fig. 16 it is shown the gamma peak of Cs-137 source at 662 KeV : it is not particularly good and this is another proof of the high hole trap density in the detector. It is not possible to improve the collection efficiency increasing the bias voltage by the presence of discharge effects and charge injection from the contacts for an electric field up to  $4 \times 10^4$  Volt/cm that worse the spectra at all energies.

## 7. - CONCLUSIONS

HgI<sub>2</sub> crystals present good performances as gamma and X ray detector in a energy range varying from 10 KeV up to 1.5 MeV and they can work at room temperature with good results, making them a good tool for dosimetric applications, in an energy range wider than ionization chambers. To improve the HgI<sub>2</sub> detector performances it is necessary to be careful at the following effects:

- to reduce the trap density that gives origin to polarization effect and decreases the charge collection.
- to reduce the reverse current, which is the principal cause of the detector noise, acting above all on a better technique of cutting the detectors from HgI<sub>2</sub> ingot, because surface stresses generate a direct increase of dark current.
- to optimize the metal semiconductor contact : it is very important to avoid dead zones under the electrodes where the charge induced by the incident radiation is not collected.
- to choose an electric chain as noiseless as possible, with a JFET as

first stage of the preamplifier ,that has only Johnson noise.

The  $HgI_2$  carrier mobility is an handicap to its employ (see Tab. 1), so we have studied the possibility of building detectors cut perpendicularly to the layers, where we have found a better hole mobility (  $19 \text{ cm}^2/\text{V sec.}$  ). But the crystals cut in this way are very fragile and the spectra analysis have not confirmed an improvement to the previous situation, probably by the worse electron mobility (  $65 \text{ cm}^2/\text{V sec.}$  ).

We are studying the possibility to build a survey dosimeter that exploits  $HgI_2$  performances as gamma and X-ray detector.

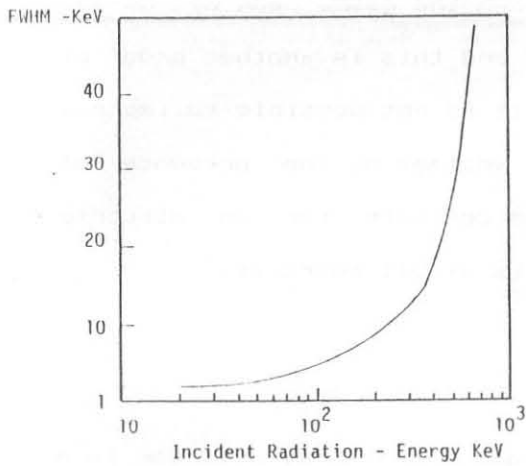


FIG.11: Behaviour of  $E_{FWHM}$  of the peak in function of the incident radiation energy  $E$ .

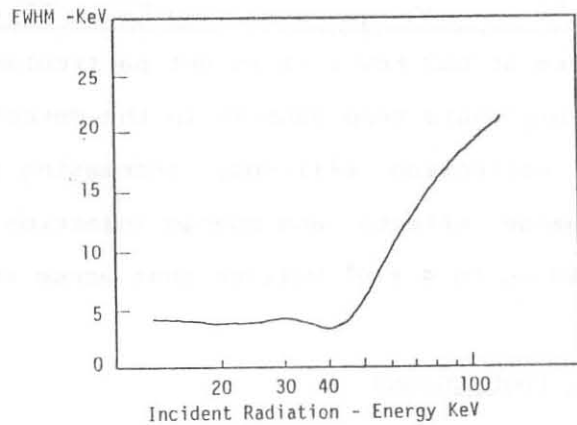


FIG.12: Theoretical calculation by Montecarlo Method of detector energy resolution  $E_{FWHM}$  as a function of radiation energy.

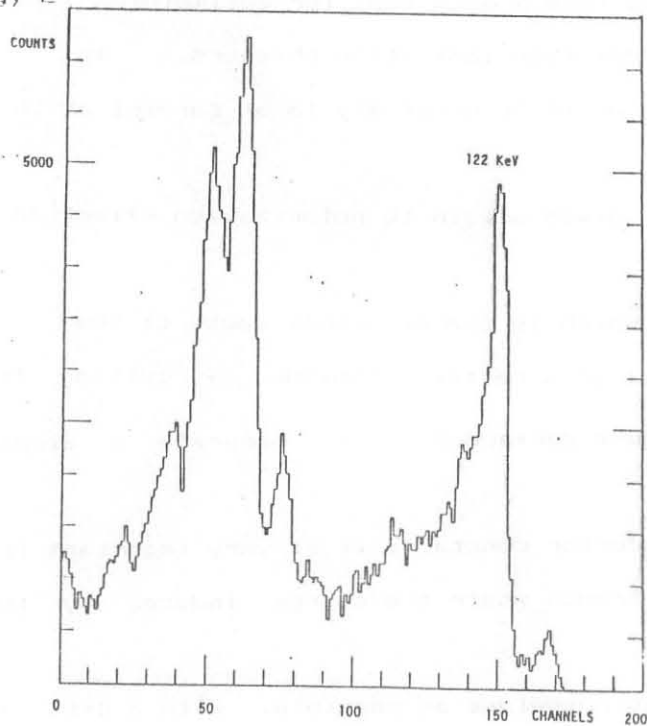


Fig.13: Co-57 Gamma source.

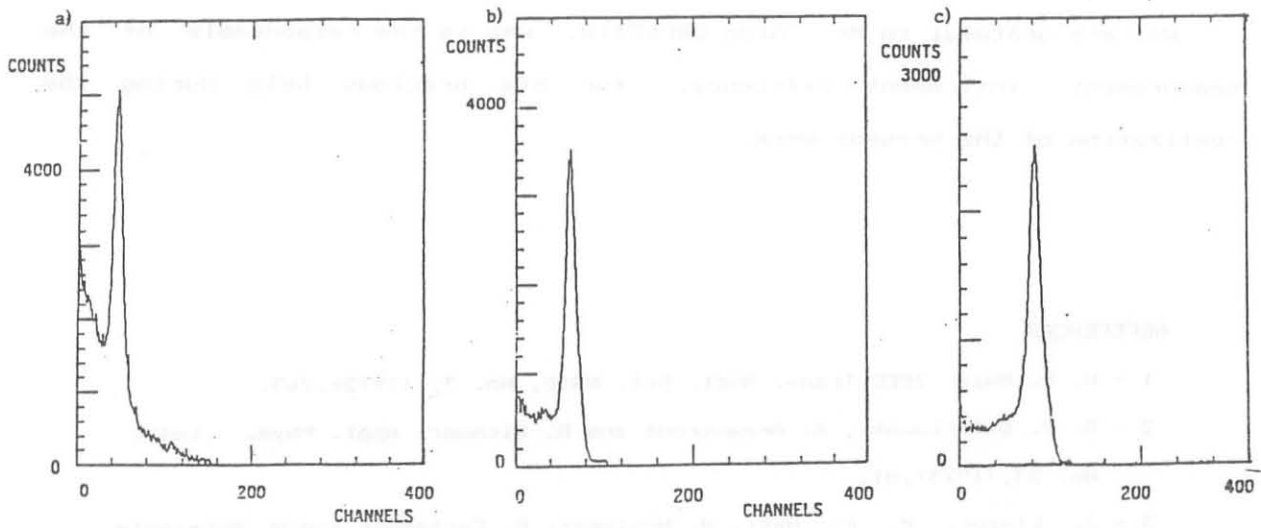


Fig. 14 : a) Rb X source  $E=13$  KeV; b) Mo X source  $E=17$  KeV; c) Ag X source  $E=22$  KeV.

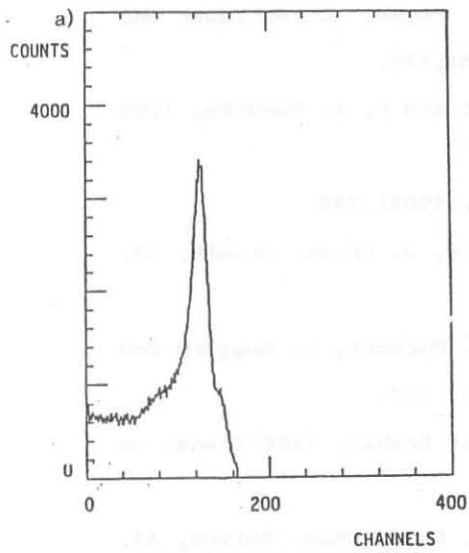


Fig.15: a) Ba X source,  $E= 32$  KeV b) Tb X source  $E= 44$  KeV.

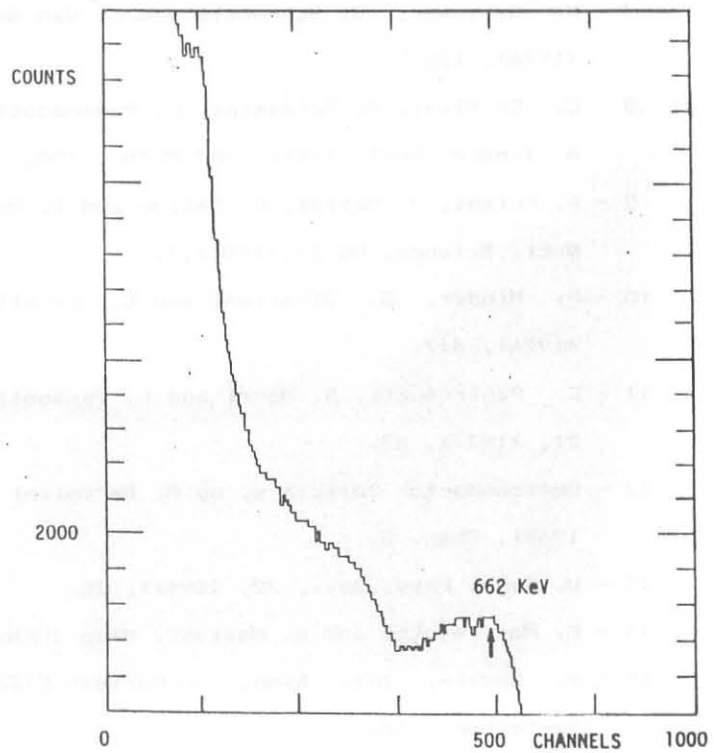
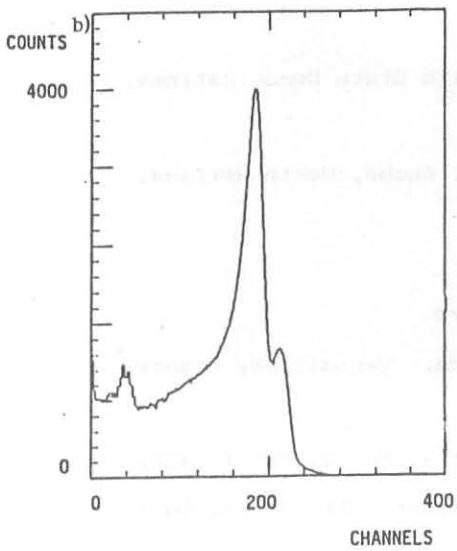


Fig.16: Cs-137 Gamma source.

ACKNOWLEDGE

We are grateful to Mr. Aldo CROSETTO, who is the responsible of the measurement instrument efficiency, for his precious help during the realization of the present work.

REFERENCES

- 1 - H. L. Malm IEEE Trans. Nucl. Sci. NS19, No. 3, (1972),263.
- 2 - S. P. Swierkowski, G. Armantrout and R. Wichner, Appl. Phys. Lett. No. 23, (1973),81.
- 3 - J. Llacer, M. K. Watt, M. Schieber, R. Carlstone and W. Schnapple, IEEE Trans. Nucl. Sci., NS 21, No. 6, (1974),305
- 4 - J. D. Ponpon, R. Stuck, P. Siffert, B. Meyer, C. Schieber and T. Schwad, IEEE Trans. Nucl. Sci., NS 22, (1975),178.
- 5 - M. Slapa, G. T. Huth, W. Seibt, M. Schiebert and P. T. Randtke, IEEE Trans. Nucl. Sci., NS 23, (1976),102.
- 6 - C. Manfredotti, Nucl. Instr. and Meth., N. 22, (1984),345
- 7 - M. Schieber, W. Schnapple and L. Van der Berg, J. Cryst. Growth, 33, (1976), 125
- 8 - C. De Blasi, S. Galassini, C. Manfredotti, G. Micocci, L. Ruggero and A. Tepore, Nucl. Instr. and Meth., 150, (1978), 103.
- 9 - A. Friant, J. Mellet, C. Saliou and T. Mohammed Brahin, IEEE Trans. on Nucl. Science, NS 27, (1980),7.
- 10 - R. Minder, G. Ottaviani and C. Canali, J. Phys. Chem. Solids, 37, (1976), 417.
- 11 - C. Manfredotti, R. Murri and L. Vasanelli, Solid State Communications, 21, (1977), 53.
- 12 - Semiconductor Detectors, by G. Bertolini and C. Coche, (North Holland, 1968), Chap. 5.
- 13 - U. Fano, Phys. Rev., 72, (1947), 26.
- 14 - C. Manfredotti and U. Nastasi, Rapp INFN/TC-83/2
- 15 - V. Radeka, Int. Symp. on Nuclear Electronics, Versailles, France, September 1968.
- 16 - G. Ottaviani and K. R. Zanio, Phys. Rev. B, Vol 4, No. 2, (1971),422.
- 17 - S. P. Swierkowski, G. A. Armantrout and R. Wichner, IEEE Trans. Nucl. Sci., NS 21, No. 1, (1974),302.